SSRG International Journal of Electrical and Electronics Engineering
ISSN: 2348-8379/ https://doi.org/10.14445/23488379/IJEEE-V11I4P101

Volume 11 Issue 4, 1-7, April 2024

Original Article

Design of Triple-Band Two-Port DR-Based MIMO Antenna with Circularly Polarization for Wireless Application

Vivek Kumar Gupta[1], Monauwer Alam[2]

[1,2]*ECE Department, Integral University, Uttar Pradesh, India.*

[1]*Corresponding Author : vivekgupta9384@gmail.com*

Received: 03 February 2024 Revised: 02 March 2024 Accepted: 01 April 2024 Published: 30 April 2024

Abstract *- In this study, a meticulously designed compact Cylindrical Dielectric Resonator Antenna (CDRA) has been comprehensively examined. This CDRA exhibits a versatile range of polarization characteristics across two distinct frequency ranges. This CDRA exhibits two noteworthy features: Firstly, it utilizes a pentagon-shaped aperture for excitation, effectively generating triple radiating modes within it, namely, $HEM_{11\delta}$, $HEM_{12\delta}$, and $HEM_{13\delta}$. Secondly, the proposed CDRA offers support for two distinct polarization features, namely linear and circular polarization. The first band spans from 3.5 to 4.1 GHz, the second band extends from 6.57 to 7.1 GHz, and the third band covers the range of 7.79 to 8.7 GHz. The antenna maintains an axial ratio below 3 dB in the second band (6.9 - 7.1 GHz) and the third band (8.35 - 8.7 GHz). This design ensures stable circular polarization, enhancing its suitability for a variety of communication applications.*

Keywords *- Circular polarization, Axial ratio, Dual-band, Cylindrical Dielectric Resonator Antenna, ECC.*

1. Introduction

Owing to fluctuations in high-frequency signal strength and the unprecedented proliferation of mobile users, there exists a compelling imperative for the progression of wireless technology. The evolution of next-generation mobile communication technology necessitates the allocation of higher spectrum frequencies and an augmentation of data rates [1]. The fulfilment of these requisites can be achieved through the utilization of Multiple Input Multiple Output (MIMO) antennas, as these sophisticated antenna systems possess the capability to deliver elevated data rates without the need for escalating power levels.

Additionally, MIMO antennas contribute to heightened spectrum efficiency, further enhancing their suitability for meeting the specified requirements [2-4]. Various types of radiators, including microstrip, slot, and Dielectric Resonator (DR) antennas, find application in the design of MIMO antennas. Notably, DR-based MIMO radiators are widely preferred due to their capacity to provide diverse radiation properties, thereby enabling higher impedance bandwidth and gain at elevated frequencies. Within the domain of DR-based MIMO, two major focal points emerge: (i) improving isolation between multiple antenna ports and (ii) manipulating the electric field orientation of the transmitted wave to generate various polarization types [5-9]. The concern regarding isolation between antenna ports holds significance, as it directly influences several key antenna parameters. This includes a substantial decrease in the signal-to-noise ratio, a noteworthy alteration in gain and efficiency, as well as changes in the gain beam-scanning property of the array. Additionally, there is a consequential reduction in data throughput attributed to the elevated value of the Envelope Correlation Coefficient (ECC) [10-17]. Circular polarization is achieved by having two perpendicular modes with equal amplitudes and a phase offset of 90 degrees (in-phase quadrature) [18].

The synergistic exploration of multiband functionality alongside circular polarization attributes stands as a prominently concentrated realm within the domain of antenna research. This prominence is attributed to two pivotal factors: firstly, its remarkable capacity to adeptly accommodate multiple frequency bands concurrently, and secondly, the inherent capacity of the receiving antenna to achieve orientation independence [19-21].

Das et al. innovatively introduced a dual-band hybrid MIMO DRA endowed with a redesigned ring-shaped aperture strategically crafted to elicit HEM11δ and TE01δ modes. The orchestrated orthogonal configurations of the antenna elements intricately contribute to realizing isolation levels that exceed the threshold of 20 dB [8]. To achieve improved isolation, Aftab et al. presented a dual-band MIMO stacked

DRA that included a defective ground plane [22]. A single-band dual-port DR-based MIMO antenna with circular polarisation characteristics and a 3-dB axial ratio bandwidth of 4.55% was recently introduced by Varshney et al. [23]. A singly fed, dual-band, Circularly Polarised (CP) antenna with a single port and a high gain value of roughly 6–8 dBi was proposed by Xiasheng et al. Although the authors were able to produce CP waves, the result is a massive physical size of 160×160×40.3 [24]. In this article, a Triple-band Two-Port CDRA with a wide range of polarization characteristics in dual-band is meticulously designed and thoroughly investigated. The pivotal modification entails the manipulation of the pentagon-shaped aperture employed for exciting the CDRA, yielding two indispensable attributes within the envisioned antenna configuration:

1. The ability to excite three hybrid radiating modes, specifically $HEM_{11\delta}$, $HEM_{12\delta}$, and $HEM_{13\delta}$.
2. The provision of diversified polarization features across different operating frequency ranges with good isolation between the ports.

The proposed article delineates distinct sections comprising (2) Antenna Geometry, (3) Analysis of the Proposed Structure, (4) Analysis of simulated and measured results, (5) Conclusion, and (6) Reference.

2. Antenna Geometry

The illustrated Figure 1 delineates the geometric characteristics of the envisioned dual-port CDRA, an extension of the single-port design. Figure 2 illustrates the proposed single-port design, including its associated feed structure. The single port CDRA is meticulously crafted from Al2O3 with specific dielectric properties (εr=9.8 and δ=0.002) and is affixed onto an FR4 glass epoxy substrate possessing its own set of dielectric constants (εr=4.4 and δ=0.002). This design configuration incorporates a ground plane positioned atop the substrate, with the microstrip line strategically situated beneath it, illustrating a well-thought-out arrangement for optimal antenna performance.

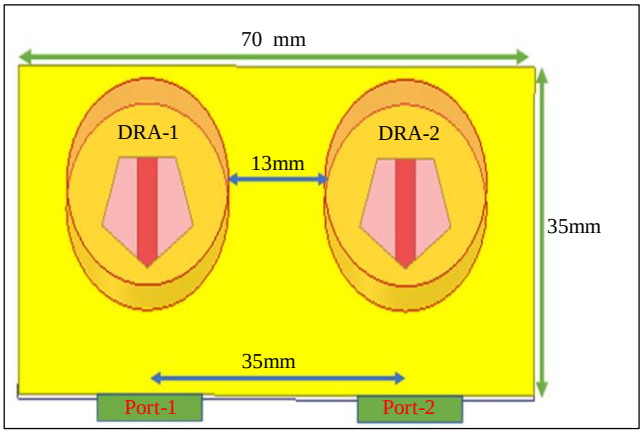

Fig. 1 Structure of proposed dual-port design

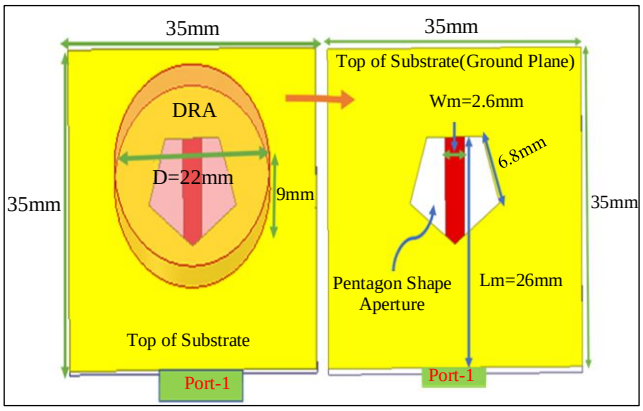

Fig. 2 Structure proposed of single port design (a) Top view single port antenna, and (b) Feed line.

3. Analysis of the Proposed Antenna

In this specific segment, a meticulous exploration of the engineered antenna is undertaken through the utilization of the CST and Ansys HFSS electromagnetic system. The comprehensive analysis of the antenna is systematically divided into two distinct sections: an in-depth examination of single-port characteristics followed by a rigorous scrutiny of double-port attributes.

3.1. Analysis of Single-Port Antenna

In Figure 3, a graphical representation of the reflection coefficient variations is provided. This figure offers clear evidence of the proposed single-port design's proficiency in operating across three well-defined frequency bands. The initial band covers frequencies ranging between 3.5 and 4.1 GHz, the subsequent band extends from 6.57 to 7.1 GHz, and the final band spans from 7.79 to 8.7 GHz.

Figure 4 provides a visual representation of the variation in axial ratio. It is readily discernible from the figure that the proposed design manifests elliptical polarization characteristics within the first frequency band, gracefully transitioning to circular polarization in the second and third bands.

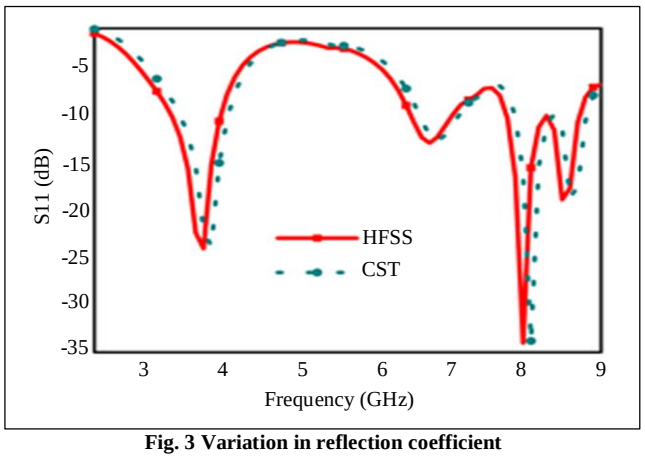

Fig. 3 Variation in reflection coefficient

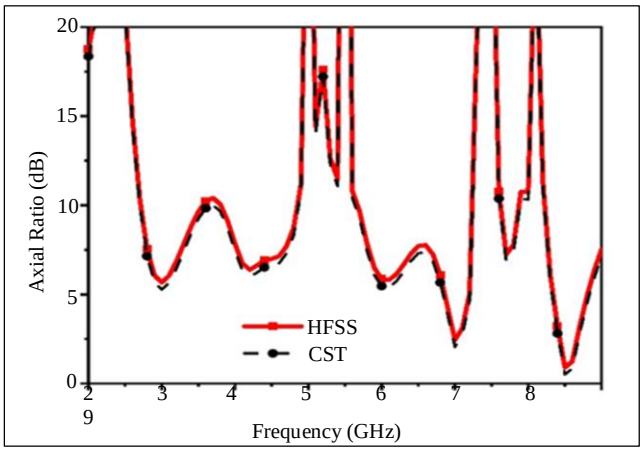

Fig. 4 Variation in axial ratio

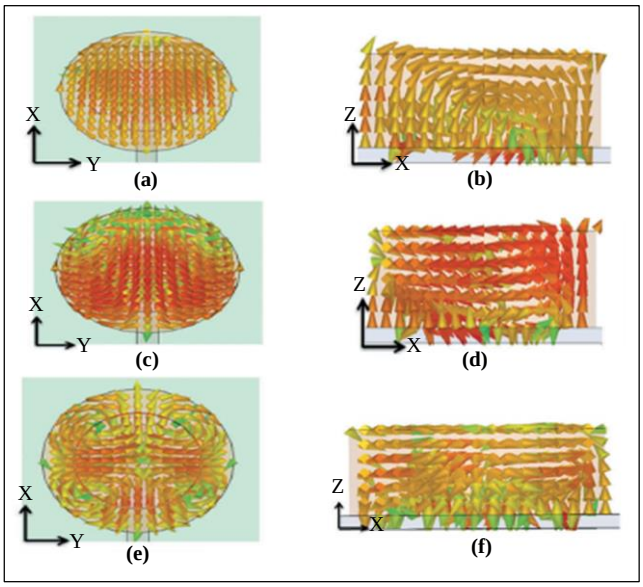

Fig. 5 Electric field variation on CDRA at different frequencies (a) Side view at 3.8GHz, (b) Top view at 3.8 GHz, (c) Side view at 6.8GHz, (d) Top view at 6.8 GHz, (e) Side view at 8.1GHz, and (f) Top view at 8.1 GHz.

Notably, the axial ratio in the proposed design consistently remains below 3 dB in the second band, spanning from 6.9 to 7.1 GHz, as well as in the third band, encompassing frequencies from 8.35 to 8.7 GHz.

This indicates excellent circular polarization performance within these frequency ranges. Figure 5 illustrates the Electric field variation on the CDRA at frequencies of 3.8 GHz, 6.8 GHz, and 8.1 GHz.

Figure 6 depicts a parametric analysis of the designed single-port radiator. It is evident from the figure that an increase in the height of the DRA leads to a discernible trend, manifesting a notable shift in resonance frequencies across both input impedance and Axial Ratio (AR) bandwidth. This observed shift is attributable to the suppression of Z-directional waves within the structural configuration of the antenna.

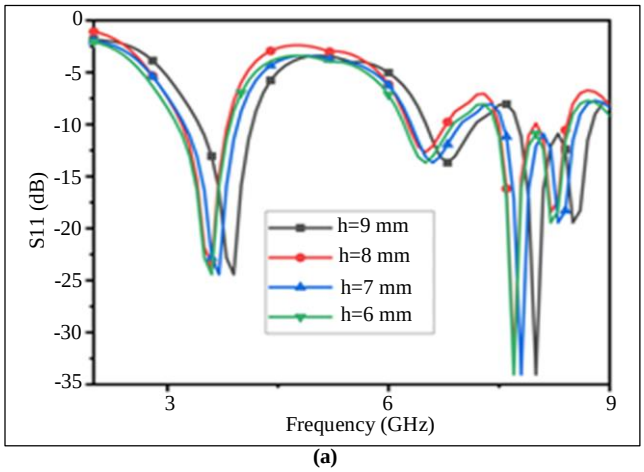

(a)

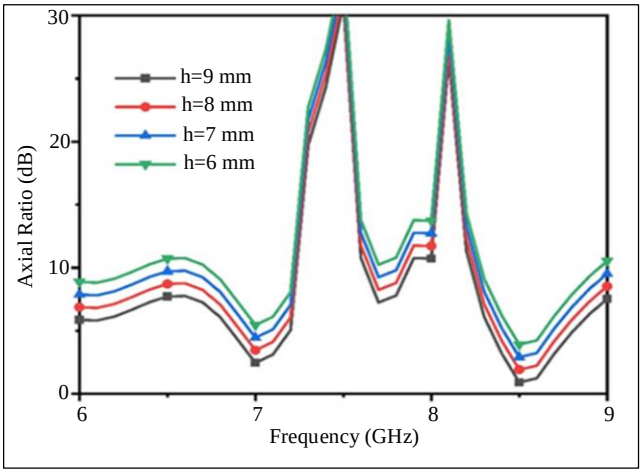

(b)

Fig. 6 Variation in S11 and axial ratio due to variation in height (a) S11 variation, and (b) Axial ratio variation.

3.2. Analysis of the Proposed Dual-Port Antenna

This section delves into the sophisticated design of the envisioned Two-port antenna, as depicted in Figure 1. This design represents an extension originating from the single-port antenna A, intricately crafted to function seamlessly within the predefined frequency range.

The subsequent analysis, illustrated in Figure 8, unveils insights into the scattering parameter. Upon meticulous scrutiny, it becomes evident that the reflection coefficient follows a remarkably similar pattern in both cases.

Notably, the mutual coupling surpasses -20 dB, underscoring its efficacy within the specified frequency range. Figure 8 illustrates the fluctuation in the Axial ratio of the envisaged dual-port antenna. It is evident from Figure 8 that the axial ratio dips below the critical threshold of 3-dB within two distinct frequency bands.

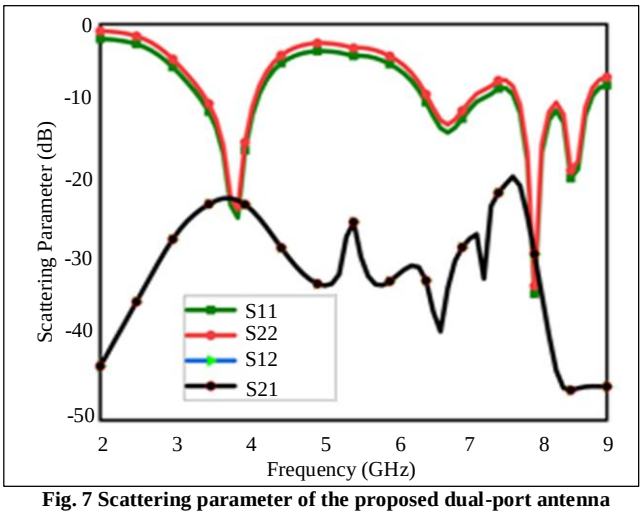

Fig. 7 Scattering parameter of the proposed dual-port antenna

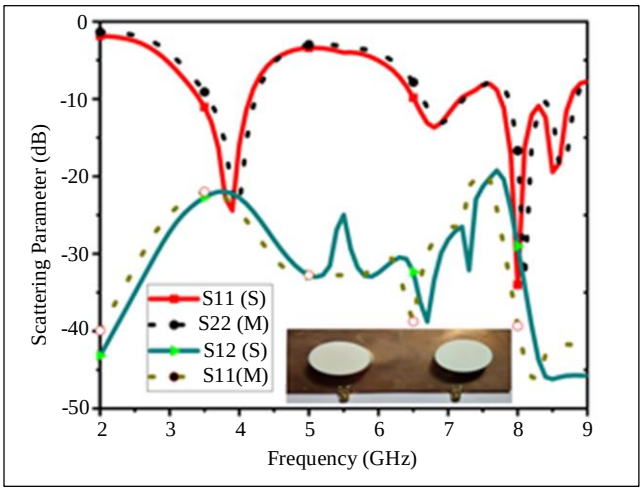

Fig. 9 illustrates the comparative analysis between the measured and simulated scattering parameters of the two-port antenna

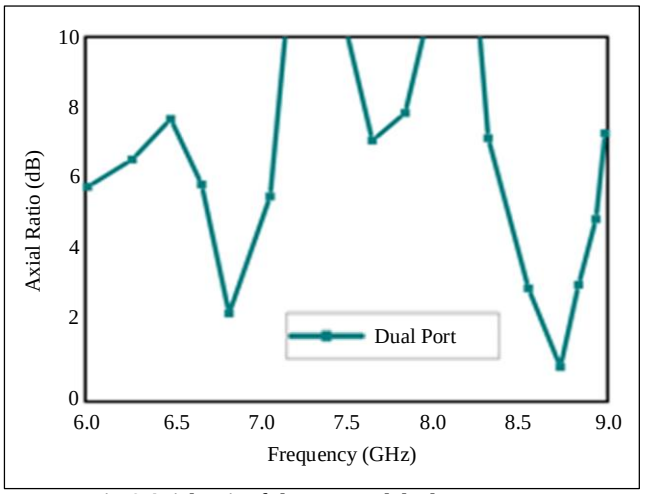

Fig. 8 Axial ratio of the proposed dual-port antenna

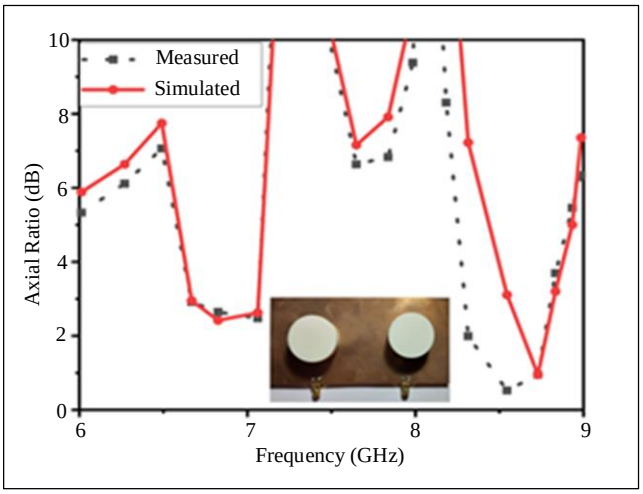

Fig. 10 Illustrates the comparative analysis between the measured and simulated axial ratio of the two-port antenna

4. Analysis of Simulated and Measured Result

To substantiate the design, a constructed Circularly Polarized (CP) antenna was subjected to construction and assessment. The reflection coefficient was precisely quantified utilizing an HP8510C network analyzer, and various additional findings were gathered through the utilization of a Satimo Startlab System. Figure 9 provides a comprehensive visualization of the comparison between the simulated and experimentally determined reflection coefficients for the prototype.

The graphical representation reveals that the -10 dB impedance bandwidths for the first band extend from 3.5 to 4.1 GHz, the second band covers a range from 6.57 to 7.1 GHz, and the third band encompasses frequencies from 7.79 to 8.7 GHz. These measurements exhibit a noteworthy alignment with their respective simulated values, indicating a high degree of agreement between the experimental and theoretical data.

In Figure 10, the depiction of the concordance between simulated and measured Axial Ratios (ARs) for the proposed antenna showcases any differences that may arise from experimental tolerances and imperfections.

Notably, the 3-dB AR bandwidths drop below 3 dB within the second band, precisely from 6.9 to 7.1 GHz, as well as in the third band, covering the range of 8.35 to 8.7 GHz.

Figure 11 provides a graphical representation of the variations in measured and simulated gain and radiation efficiency across different frequency ranges.

Notably, the gain remains relatively stable at approximately four dBi within the 3.5 to 4.1 GHz range, experiences a significant surge to approximately 12 dBi between 6.57 to 7.1 GHz, and further elevates to around 16 dBi within the frequency spectrum of 7.79 to 8.7 GHz.

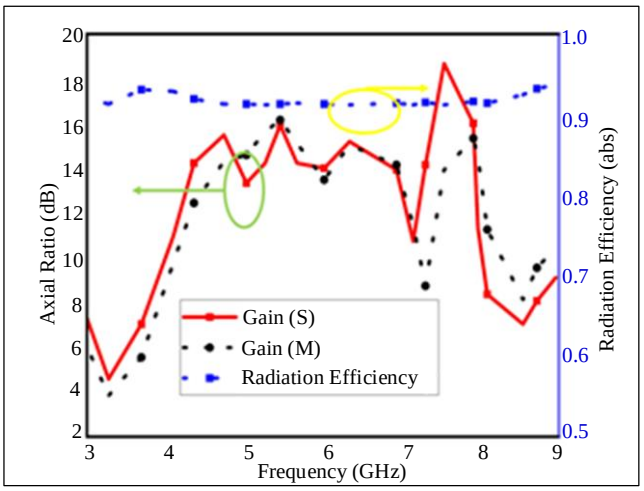

Fig. 11 illustrates the comparative analysis between the measured and simulated gain and simulated radiation efficiency of the two-port antenna

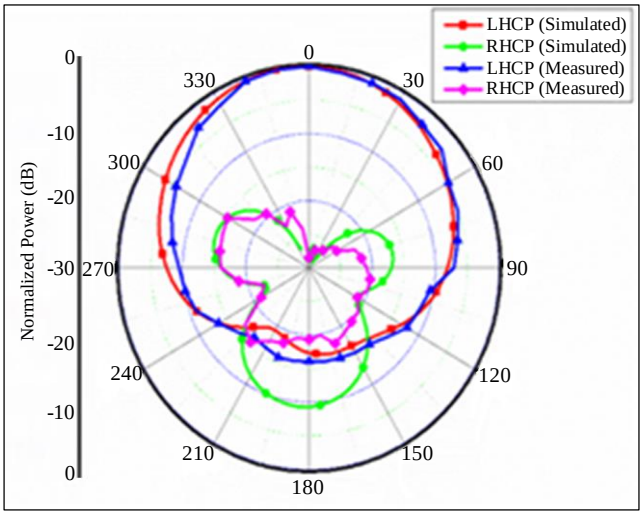

(a)

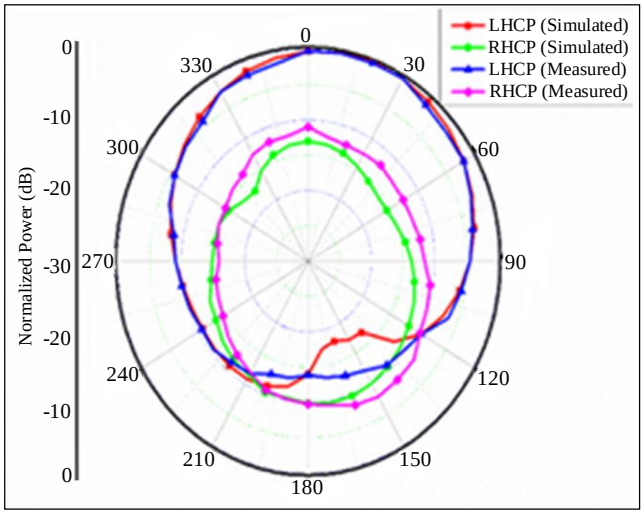

(b)

Fig. 12 Radiation Pattern in XZ-Plane (a) At frequency 6.8 GHz, and (b) At frequency 8.5 GHz.

Two notable observations are derived from Figure 12: firstly, the radiator, as designed, functions as Left-Handed Circularly Polarized (LHCP), with LHCP exhibiting greater dominance over Right-Handed Circularly Polarized (RHCP); and secondly, a broadside pattern is achieved from both ports.

To ameliorate the impacts of detrimental interference stemming from multipath fading, it is imperative to deploy an appropriate concept of diversity scheme. The efficacy of the proposed dual-port radiator can be evaluated through three foundational performance metrics: the Envelope Correlation Coefficient (ECC), Directive Gain (DG), and Channel Capacity Loss (CCL).

ECC serves as a crucial metric for quantifying interference between a pair of radiators. Ranging from 0 to 1, ECC values offer insights into the extent of overlap within radiation patterns. A minimum ECC value signifies pristine separation, indicating negligible interference. Conversely, an ECC of 1 signal pronounced overlap, indicative of compromised antenna performance due to radiation pattern convergence. The optimal ECC target lies below 0.05, highlighting the ideal balance between minimal interference and maximal antenna efficacy [18]. The determination of the ECC value can be accomplished through the utilization of Equation 1.

$$ECC=\left\{\frac{|S_{11}*S_{12}+S_{21}*S_{22}|^2}{[1-|S_{11}|^2-|S_{21}|^2][1-|S_{22}|^2-|S_{12}|^2]}\right\} \quad (1)$$

DG stands as a critical metric in assessing the efficacy of MIMO antennas. Equation 2 delineates an approximate correlation between ECC and DG. An optimal DG value of 10 is deemed ideal; nonetheless, a range surpassing 6 denotes a commendable level of performance.

$$DG=10*[1-|ECC^2|]^{0.5} \quad (2)$$

Channel Capacity Loss (CCL) elucidates the diminishment in information transmission rate resultant from correlation's impact. In the context of N-port MIMO systems, CCL can be quantified through the utilization of the equations [3-6].

$$CCL=-\log_2 \det[\psi^R] \quad (3)$$

$$\psi^R=\begin{pmatrix}\rho_{11} & \rho_{12}\\ \rho_{21} & \rho_{22}\end{pmatrix} \quad (4)$$

$$\rho_{ij}=1-\{|S_{jj}|^2+|S_{jk}|^2\} \quad (5)$$

$$\rho_{jk}=-\{S_{jj}^**S_{jk}+S_{kj}^**S_{kk}\} \quad (6)$$

Figure 13 illustrates the variation in measured/simulated Error Correction Coding (ECC) and Directivity Gain (DG) for the designed radiator.

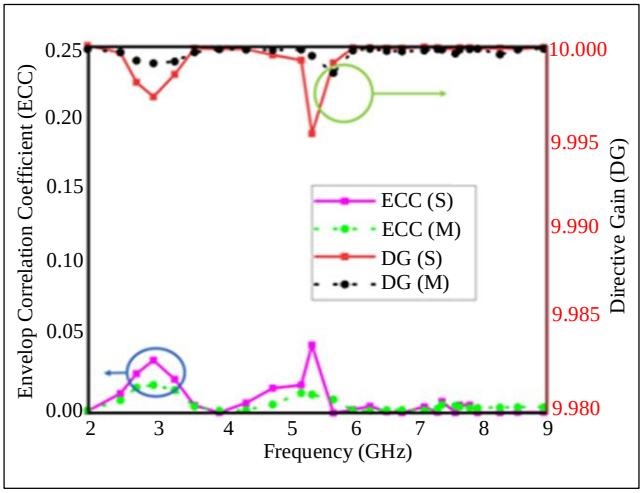

Fig. 13 illustrates the comparative analysis between the measured and simulated DG and ECC

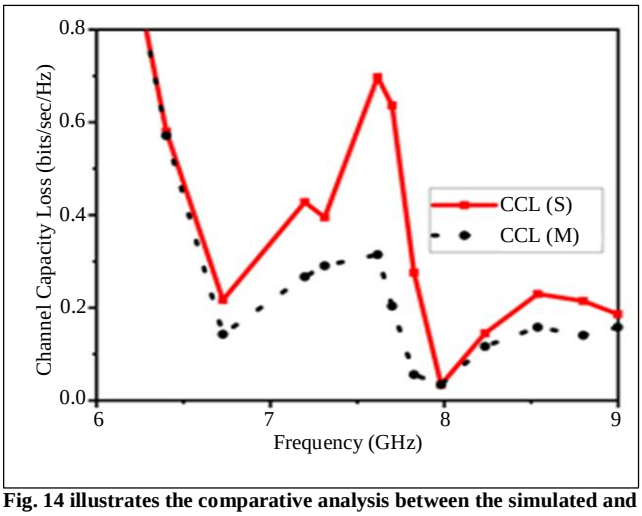

Fig. 14 illustrates the comparative analysis between the simulated and measured CCL

Analysis of Figure 13 reveals an ECC value consistently below 0.3, accompanied by a diversity gain of approximately 10.0 dB across the operational frequency spectrum. Figure 14 depicts the fluctuation in CCL.

Upon analysis, it becomes evident that the CCL values consistently fall below the designated threshold of 0.5 throughout the operational frequency spectrum. A comparative analysis of the performance of the proposed DR-based MIMO radiator against other existing DR-based radiators was provided. From that, it becomes apparent that the designed radiator exhibits superior overall performance in comparison to other existing MIMO radiators.

5. Conclusion

In this communication, a meticulously designed compact Cylindrical Dielectric Resonator Antenna (CDRA) has been comprehensively explored, revealing a rich array of polarization characteristics within two discrete frequency ranges. The proposed design impressively extends its operational range across three well-defined frequency bands: 3.5 to 4.1 GHz, 6.57 to 7.1 GHz, and 7.79 to 8.7 GHz.

In the first band, it showcases prominent linear polarization attributes while seamlessly transitioning to distinct circular polarization features within the second and third bands, with Axial Ratio (AR) bandwidths spanning the frequency ranges of 6.9 to 7.1 GHz and 8.35 to 8.7 GHz, respectively.

Further, the conversion of a single-port design into a dual-port MIMO DRA demonstrates promising outcomes, as evidenced by the favorable values observed in diversity parameters.

Acknowledgments

All authors express their heartfelt gratitude to Integral University, Lucknow, for graciously assigning manuscript number 1U/R&D/2023-MCN0002258, thus enabling the progression of our current research endeavors.

References

[1] Erik G. Larsson et al., "Massive MIMO for Next Generation Wireless Systems," *IEEE Communications Magazine*, vol. 52, no. 2, pp. 186-195, 2014. [CrossRef] [Google Scholar] [Publisher Link]

[2] Abhimanyu Yadav et al., "Two-Port Metasurface-Loaded Circularly Polarized Al_2O_3 Ceramic-Based Filtering Antenna for 2.5/2.6 GHz Band," *Journal of Electronic Materials*, vol. 52, pp. 8141-8150, 2023. [CrossRef] [Google Scholar] [Publisher Link]

[3] M.A. Jensen, and J.W. Wallace, "A Review of Antennas and Propagation for MIMO Wireless Communications," *IEEE Transactions on Antennas and Propagation*, vol. 52, no. 11, pp. 2810-2824, 2004. [CrossRef] [Google Scholar] [Publisher Link]

[4] Srinivas Guthi, and Vakula Damera, "High Gain and Broadband Circularly Polarized Antenna Using Metasurface and CPW fed L-Shaped Aperture, "*AEU-International Journal of Electronics and Communications*, vol. 146, 2022. [CrossRef] [Google Scholar] [Publisher Link]

[5] Mohammad S. Sharawi et al., "A Dual-Element Dual-Band MIMO Antenna System with Enhanced Isolation for Mobile Terminals," *IEEE Antennas and Wireless Propagation Letters*, vol. 11, pp.1006-1009, 2012. [CrossRef] [Google Scholar] [Publisher Link]

[6] Muhammad Umar Khan, and Mohammad S. Sharawi, "A Dual-Band Microstrip Annular Slot-Based MIMO Antenna System," *Microwave and Optical Technology Letters*, vol. 57, no. 2, pp. 360-364, 2015. [CrossRef] [Google Scholar] [Publisher Link]

[7] Abhimanyu Yadav, Manish Tiwari, and Anand Sharma, "Dual-Band Quasi-Isotropic Dielectric Resonator-Based Filtering Antenna for IoT Applications," *Journal of Electronic Materials*, vol. 52, no. 2, pp. 1590-1598, 2023. [CrossRef] [Google Scholar] [Publisher Link]

[8] Gourab Das, Anand Sharma, and Ravi Kumar Gangwar, "Dielectric Resonator-Based Two-Element MIMO Antenna System with Dual Band Characteristics," *IET Microwaves, Antennas & Propagation*, vol. 12, no. 5, pp. 734-741, 2018. [CrossRef] [Google Scholar] [Publisher Link]

[9] Huy-Hung Tran et al., "Isolation in Dual-Sense CP MIMO Antennas and Role of Decoupling Structures," *IEEE Antennas and Wireless Propagation Letters*, vol. 21, no. 6, pp. 1203-1207, 2022. [CrossRef] [Google Scholar] [Publisher Link]

[10] H. Steyskal, and J.S. Herd, "Mutual Coupling Compensation in Small Array Antennas," *IEEE Transactions on Antennas and Propagation*, vol. 38, no. 12, pp. 1971-1975, 1990. [CrossRef] [Google Scholar] [Publisher Link]

[11] Pawandeep S. Taluja, and Brian L. Hughes, "Diversity Limits of Compact Broadband Multi-Antenna Systems," *IEEE Journal on Selected Areas in Communications*, vol. 31, no. 2, pp. 326-337, 2013. [CrossRef] [Google Scholar] [Publisher Link]

[12] Saou-Wen Su, Cheng-Tse Lee, and Fa-Shian Chang, "Printed MIMO-Antenna System Using Neutralization-Line Technique for Wireless USB-Dongle Applications," *IEEE Transactions on Antennas and Propagation*, vol. 60, no. 2, pp. 456-463, 2012. [CrossRef] [Google Scholar] [Publisher Link]

[13] Luyu Zhao, and Ke-Li Wu, "A Decoupling Technique for Four-Element Symmetric Arrays with Reactively Loaded Dummy Elements," *IEEE Transactions on Antennas and Propagation*, vol. 62, no. 8, pp. 4416-4421, 2014. [CrossRef] [Google Scholar] [Publisher Link]

[14] Lu Lu et al., "An Overview of Massive MIMO: Benefits and Challenges," *IEEE Journal of Selected Topics in Signal Processing*, vol. 8, no. 5, pp. 742-758, 2014. [CrossRef] [Google Scholar] [Publisher Link]

[15] Buon Kiong Lau, and Jørgen Bach Andersen, "Simple and Efficient Decoupling of Compact Arrays with Parasitic Scatterers," *IEEE Transactions on Antennas and Propagation*, vol. 60, no. 2, pp. 464-472, 2012. [CrossRef] [Google Scholar] [Publisher Link]

[16] D. Pozar, "Considerations for Millimeter Wave Printed Antennas," *IEEE Transactions on Antennas and Propagation*, vol. 31, no. 5, pp. 740-747, 1983. [CrossRef] [Google Scholar] [Publisher Link]

[17] Yan Wang, and Zhengwei Du, "A Wideband Printed Dual-Antenna with Three Neutralization Lines for Mobile Terminals," *IEEE Transactions on Antennas and Propagation*, vol. 62, no. 3, pp. 1495-1500, 2014. [CrossRef] [Google Scholar] [Publisher Link]

[18] Chih-Yu Huang, and Ching-Wei Ling, "Frequency-Adjustable Circularly Polarised Dielectric Resonator Antenna with Slotted Ground Plane," *Electronics Letters*, vol. 39, no. 14, pp. 1030-1031, 2003. [CrossRef] [Google Scholar] [Publisher Link]

[19] Constantine A. Balanis, *Antenna Theory: Analysis and Design*, 4th ed., John Wiley & Sons, pp. 1-1104, 2016. [Google Scholar] [Publisher Link]

[20] Deepak Batra, and Sanjay Sharma, "Dual Band Dielectric Resonator Antenna for Wireless Application," *International Journal of Electronics*, vol. 99, no. 9, pp. 1323-1331, 2012. [CrossRef] [Google Scholar] [Publisher Link]

[21] Z. Rahimian, S. Nikmehr, and A. pourziad, "Circularly Polarized Rectangular Dielectric Resonator Antennas with Branch-Line Coupler for Wideband Applications," *AEU-International Journal of Electronics and Communications*, vol. 69, no. 1, pp. 169-175, 2015. [CrossRef] [Google Scholar] [Publisher Link]

[22] Aftab Ahmad Khan et al., "Dual-Band MIMO Dielectric Resonator Antenna for WiMAX/WLAN Applications," *IET Microwaves, Antennas & Propagation*, vol. 11, no. 1, pp. 113-120, 2017. [CrossRef] [Google Scholar] [Publisher Link]

[23] Gaurav Varshney et al., "Circularly Polarized Two-Port MIMO Dielectric Resonator Antenna," *Progress in Electromagnetics Research M*, vol. 91, pp. 19-28, 2020. [CrossRef] [Google Scholar] [Publisher Link]

[24] Xiaosheng Fang, Kwok Wa Leung, and Eng Hock Lim, "Singly-Fed Dual-Band Circularly Polarized Dielectric Resonator Antenna," *IEEE Antennas and Wireless Propagation Letters*, vol. 13, pp. 995-998, 2014. [CrossRef] [Google Scholar] [Publisher Link]